

THERMAL X-RAY EMISSION AND COSMIC RAY PRODUCTION IN YOUNG SUPERNOVA REMNANTS

ANNE DECOURCHELLE¹, DONALD C. ELLISON², AND JEAN BALLET¹

Submitted to The Astrophysical Journal Letters

ABSTRACT

We have developed a simple model to investigate the modifications of the hydrodynamics and non-equilibrium ionization X-ray emission in young supernova remnants due to nonlinear particle acceleration. In nonlinear, diffusive shock acceleration, the heating of the gas to X-ray emitting temperatures is strongly coupled to the acceleration of cosmic ray ions. If the acceleration is efficient and a significant fraction of the shock ram energy ends up in cosmic rays, compression ratios will be higher and the shocked temperature lower than test-particle, Rankine-Hugoniot relations predict. In this Letter, we show that typical parameters of young supernova remnants should result in significant nonlinear acceleration, which strongly modifies the hydrodynamics and consequently the thermal X-ray emission. We illustrate how particle acceleration impacts the interpretation of X-ray data using the X-ray spectra of Kepler's remnant, observed by *ASCA* and *RXTE*. We show that thermal X-ray emission provides important constraints on the efficiency of particle acceleration, in complement to nonthermal emission. X-ray data from *Chandra* and *XMM Newton*, plus radio observations, will be essential to quantify nonlinear effects.

Subject headings: Supernova remnants — acceleration of particles — hydrodynamics — X-rays: ISM — ISM: individual (Kepler) — ISM: abundances

1. INTRODUCTION

The strong forward and reverse shocks in young supernova remnants (SNRs) heat the ambient interstellar medium (ISM) and supernova ejecta material to X-ray emitting temperatures. This X-ray emission contains information on the supernova (e.g., type, explosion energy, mass and composition of ejecta) and on the nature of the ambient medium (e.g., uniform, stellar wind).

In addition to heating the plasma, the forward and reverse shocks are thought to accelerate some fraction of the shocked material to cosmic ray energies. A large body of evidence suggests that this acceleration can be quite efficient with as much as 50% of the ram kinetic energy of the ejecta being placed in relativistic particles and removed from the thermal plasma (e.g., Blandford & Eichler 1987; Jones & Ellison 1991; Kang & Jones 1991; Berezhko, Ksenofontov, & Petukhov 1999). Some early work investigated its observational impact (Heavens 1984, Boulares & Cox 1988, Dorfi & Böhringer 1993). However, despite the expected efficiency of shock acceleration, the modeling and interpretation of X-ray observation from SNRs are generally done assuming that the shocks *do not* place a significant fraction of their energy in cosmic rays.

The recent discovery of nonthermal X-ray emission in shell-like SNRs like SN1006 (Koyama et al. 1995), Cas A (Allen et al. 1997), G347.3-0.5 (Slane et al. 1999) and RCW86 (Borkowski et al. 2000) has shown that SNR shocks do accelerate electrons to TeV energies and supports the case for efficient proton acceleration and the necessity of including its effects in the modeling of thermal X-ray emission.

Besides providing a more self-consistent SNR model, X-ray models of cosmic ray modified SNRs provide a test of the fundamental assumption that SNRs are the primary sources of galactic cosmic ray ions. Since shocks put

more energy into accelerated ions than electrons, nonlinear effects seen in X-ray emission will be evidence for the efficient shock acceleration of ions as well.

Here, we investigate the effects of efficient particle acceleration on the hydrodynamics and thermal X-ray emission of young SNRs. We have developed a model which couples self-similar hydrodynamics (Chevalier 1983) to nonlinear diffusive shock acceleration (Berezhko & Ellison 1999; Berezhko et al. 1999; Ellison, Berezhko, & Baring 2000), and X-ray emission including non-equilibrium ionization effects (Decourchelle & Ballet 1994). We show that a modified self-similar approach is relevant in most cases and compare it to the standard unmodified test-particle case.

2. NONLINEAR SHOCK ACCELERATION

There is convincing direct and indirect evidence from spacecraft observations and plasma simulations that collisionless shocks are efficient nonlinear accelerators. Consequently, they self-generate magnetic turbulence and develop a smooth shock precursor (e.g., Drury 1983; Blandford & Eichler 1987; Jones & Ellison 1991; Achterberg, Blandford, & Reynolds 1994; Terasawa et al. 1999; Ellison et al. 2000). When the acceleration is nonlinear, the shock compression ratio increases and the shocked temperature decreases compared to test-particle values. The entire proton spectrum must be accounted for self-consistently with a non-thermal tail connecting the quasi-thermal population to the energetic one; any change in the relativistic population must impact the thermal population. In contrast, the slope and normalization of test-particle power laws can be changed without changing the temperature and density of the shock heated gas. A complete description of nonlinear effects and the model used here is given in Berezhko & Ellison (1999), Ellison et al. (2000), and Ellison (2000).

¹Service d'Astrophysique, L'Orme des Merisiers, CE-Saclay, 91191 Gif-sur-Yvette, CEDEX France; E-mail: adecourchelle@cea.fr, jballot@cea.fr

²Department of Physics, North Carolina State University, Box 8202, Raleigh NC 27695, U.S.A.; E-mail: don_ellison@ncsu.edu

3. MODIFIED HYDRODYNAMIC MODEL

3.1. Model

The evolution of young SNRs can be described by self-similar solutions (Chevalier 1982; Nadezhin 1985) provided that the initial density profiles in the ejecta and in the ambient medium have power law density distributions, respectively $\rho = g^n r^{-n} t^{n-3}$ (with $n > 5$) and $\rho = q r^{-s}$ (with $s < 3$), where r is the radius, t the SNR age and g and q are constant. The effects of cosmic ray pressure on SNR dynamics were first considered by Chevalier (1983) using a two-fluid, self-similar solution with a thermal gas (adiabatic index $\gamma = 5/3$) and a relativistic gas ($\gamma = 4/3$) having an arbitrary constant fraction of the total energy. Here, we use Chevalier's (1983) solutions for driven waves but with boundary conditions calculated from the shock acceleration model from Berezhko & Ellison (1999).

As a function of shock velocity, V_s , ambient density, ρ_0 , unshocked magnetic field, B_0 , and ambient temperature T_0 , as well as the maximum particle energy, E_{\max} ,³ and injection efficiency, $\eta_{\text{inj},p}$ (i.e., the fraction of protons with superthermal energies), the nonlinear model yields downstream values for the density and pressures in the thermal and relativistic gases, at the forward and reverse shocks. Alfvén wave heating in the precursor is used, reducing the efficiency compared to adiabatic heating. Starting with the unmodified solutions at a given age, we iterate until the modified solutions and nonlinear boundary conditions are satisfied.

Our solutions neglect cosmic ray diffusion (assuming they are spatially coupled to the gas, which is an excellent approximation for all but the highest energy particles), and assume that both the compression ratio and the relativistic to total pressure ratio are independent of time at the shock fronts, which is required for self-similarity to be valid.

Everywhere we take $n = 9$, $s = 0$, $T_0 = 10^4$ K, and equal values of $\eta_{\text{inj},p}$ and η_{mfp} at the forward and reverse shocks. For the examples given in Section 3, we use: $g = 3.4 \cdot 10^9$ CGS (which gives $E_{\text{SN}}(M_{\odot}/M_{\text{ej}})^{2/3} = 0.53 \cdot 10^{51}$ erg) $q = \rho_0 = 0.42 \text{ amu/cm}^3$, $B_0 = 5 \mu\text{G}$ and $\eta_{\text{mfp}} = 1$.

3.2. Validity of the self-similar approach

We can *a posteriori* determine the validity of the self-similar assumption, by examining the variation versus time of the compression ratio and relativistic to total pressure ratio, at the reverse shock (RS) and at the forward shock (FS). As seen in Figure 1, these ratios are nearly constant for injection parameters $\eta_{\text{inj},p} \gtrsim 2 \cdot 10^{-4}$ and negligible for $\eta_{\text{inj},p} \lesssim 10^{-5}$, so that the self-similar solutions are well justified in these cases.

For values of $\eta_{\text{inj},p} \lesssim 2 \times 10^{-4}$, unmodified solutions can occur at very high sonic Mach numbers M_s (i.e., early ages) which show a rapid transition to nonlinear solutions as M_s drops (see Berezhko & Ellison 1999). The self-similar approach is valid if this rapid transition occurs at an early stage compared to the age of the SNR.

3.3. Results on the dynamics

Figure 2 shows the density and temperature as a function of radius for various values of $\eta_{\text{inj},p}$. As $\eta_{\text{inj},p}$

increases, the compression ratio becomes higher (up to 15 here instead of 4), while the shocked temperature drops (nearly a factor of 10 between the test-particle result and $\eta_{\text{inj},p} = 10^{-4}$). Such trends were expected from Chevalier (1983), but the actual nonlinear effects lead to larger modifications because of the influence of particle escape: the maximum compression ratio is no longer limited to 7, but can rise, in principle, to infinite values.

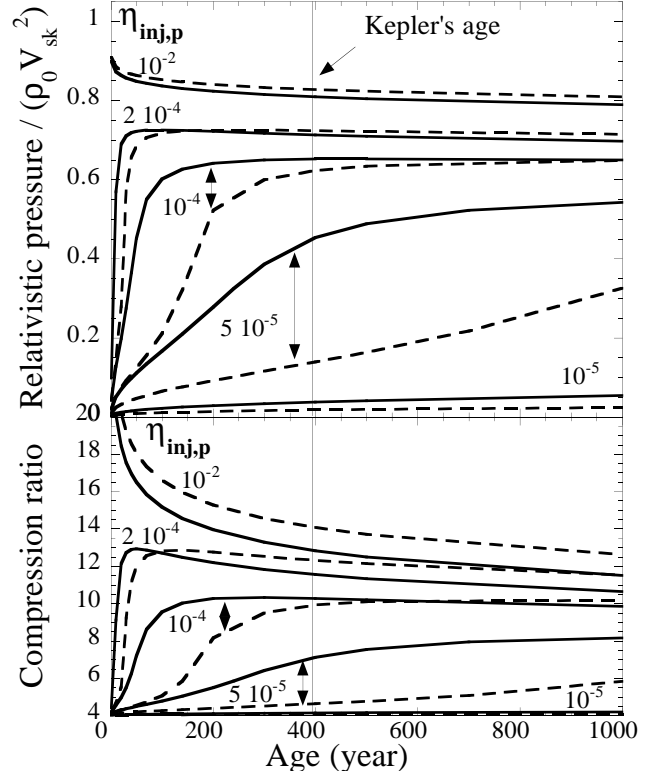


FIG. 1.— As a function of remnant age for different values of $\eta_{\text{inj},p}$, we have represented (top panel) the fraction of pressure in relativistic particles and (lower panel) the compression ratio in the forward shock (dashed curves) and in the reverse shock (solid curves).

Notably, these modifications occur for $\eta_{\text{inj},p} \gtrsim 5 \times 10^{-5}$, considerably lower than that deduced for the Earth's bow shock and from plasma simulations (i.e., $\eta_{\text{inj},p} \sim 10^{-3}$; Ellison et al. 1993). For standard values of the upstream density and magnetic field, it seems inescapable that young SNRs will experience efficient acceleration and strong modification. Table 1 gives the relative fractions of kinetic, E_{kin} , thermal, E_{th} , cosmic ray, E_{cr} , and escaped energy, E_{esc} , summed over the shocked ejecta and the shocked ambient medium. An important fraction of the energy can be carried off by escaping particles. Note that in young SNRs, the total energy in the shocked region increases with time as more and more ejecta is being shocked.

Cosmic ray modified dynamics lead to a thinner interaction region between the forward and reverse shocks and much larger density and pressure gradients. This suggests that the growth of hydrodynamic instabilities in the shocked material near the contact discontinuity will be

³ E_{\max} is determined from the shock radius, age, and diffusive mean free path, $\lambda = \eta_{\text{mfp}} r_g$, where η_{mfp} is a constant and r_g is the gyroradius (e.g., Ellison, Berezhko, & Baring 2000).

faster than otherwise. With a forward shock closer to the contact discontinuity, this may help these turbulent effects extend to the forward shock and beyond.

Equally important, the higher densities and lower temperatures will lead to more rapid Coulomb equilibration than expected in a test-particle case. Our preliminary estimates show that full equipartition between electrons and ions is likely to be achieved in the shocked ejecta.

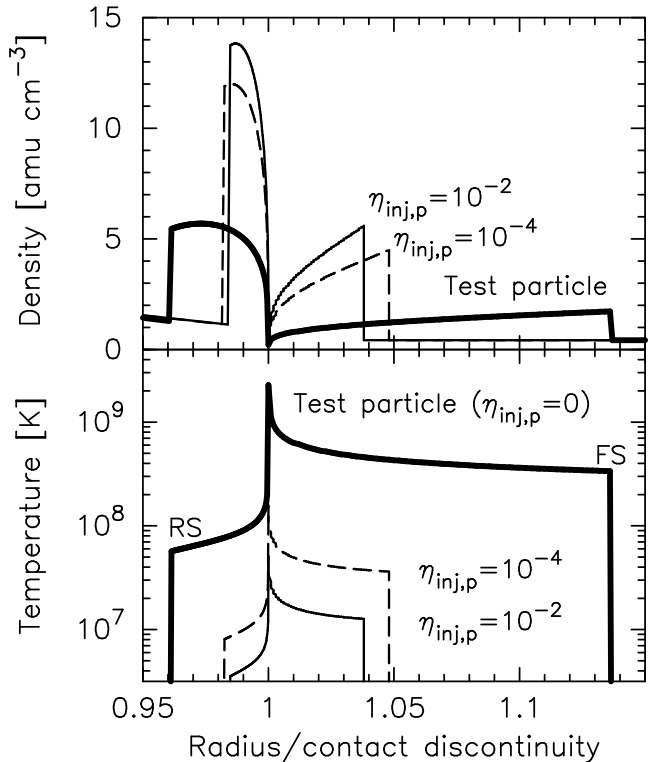


FIG. 2.— Density and temperature versus radius for different values of the injection efficiency.

3.4. Velocity versus shock temperature

Table 1. Temperature-Velocity Relation and energy fractions

$\eta_{\text{inj,p}}$	x	E_{kin}	E_{th}	E_{cr}	E_{esc}
RS	10^{-5}	0.17	0.85	0.13	0.01
	10^{-4}	0.02	0.80	0.02	0.08
	10^{-2}	0.01	0.78	0.01	0.08
FS	10^{-5}	0.18	0.48	0.48	0.03
	10^{-4}	0.02	0.42	0.04	0.26
	10^{-2}	0.01	0.41	0.01	0.33

We emphasize that when particle acceleration is efficient, the relation between the shock velocity and the mean post-shock temperature of the shocked gas is no longer approximated by the expression for a strong test-particle shock, i.e., $x = [1/(\mu m_H)] (kT_s/V_s^2) \neq 3/16$. Here μm_H is the mean particle mass and T_s is the post-shock temperature. Table 1 shows how x drops well below $3/16$ for large values of $\eta_{\text{inj,p}}$, and indicates that shock velocities derived from a measured T_s may be underestimated by a large factor. Independent measurements of V_s and T_s provide strong constraints on the amount of energy going into relativistic particles. This was shown using *Chandra* observations of E0102.2-7219 SNR, by Hughes, Rakowski, & Decourchelle (2000), who concluded that the low observed post-shock electron temperature combined

with the high observed shock velocity could only be understood if a large fraction ($\simeq 70\%$) of the shock ram energy went into cosmic rays.

4. INTERPRETATION OF X-RAY THERMAL SPECTRA

The increase in shocked density and decrease in shocked temperature from nonlinear effects, strongly impact the thermal X-ray emission. Compared to test-particle models, we predict that regions in young SNRs undergoing efficient acceleration will have a lower temperature, more intense thermal X-ray emission (due to the larger emission integral $\int n_e^2 dV$ and lower temperature), and a faster ionization timescale. In older remnants, the temperature should drop below X-ray emitting values earlier.

We have coupled our modified hydrodynamics model to the calculation of the non-equilibrium ionization and thermal X-ray emission. The ionization and recombination rates have been taken from Arnaud & Rothenflug (1985) and Arnaud & Raymond (1992). The X-ray emission code is from Mewe, Gronenschild, & Van den Oord (1985) and Mewe, Lemen, & Van den Oord (1986). The abundances in the interstellar medium are taken to be solar (Meyer 1985). We assume full equipartition between the electrons and ions ($T_e = T_i$) and neglect any contribution from the superthermal electrons to the ionization or line excitation. For efficient shock acceleration, this may be important and we are investigating these effects (Porquet et al. 2000).

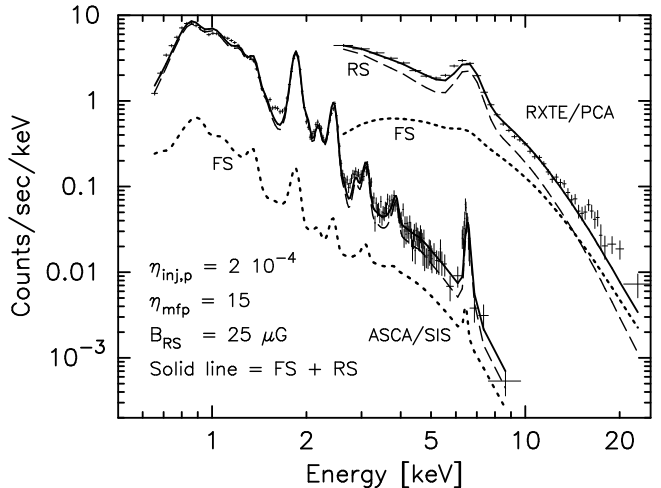


FIG. 3.— Best-fit model to the spectra of Kepler's SNR. The contribution from the shocked ejecta (RS) is shown with dashed lines, the shocked ambient matter (FS) is shown with dotted lines, and the sum is shown with solid lines.

As an indication of how the interpretation of X-ray data depends on acceleration efficiency, we model the X-ray observations of Kepler's SNR obtained over a broad energy range with *ASCA* (Kinugasa & Tsunemi 1999) and *RXTE* (Decourchelle & Petre 1999; Decourchelle et al. 2000). For several values of $\eta_{\text{inj,p}}$, we keep the acceleration parameters η_{mfp} and B_0 fixed and adjust the SNR parameters to fit the observed spectra, which are dominated by the emission from the shocked ejecta as shown in Figure 3. All values of $\eta_{\text{inj,p}}$ yield similar values for the reduced chi-squared (~ 4), the ionization timescale, the reverse shock temperature ~ 3 keV, the hydrogen column density $\sim 4 \cdot 10^{21} \text{ cm}^{-2}$, and oversolar abundances of heavy elements in the shocked

Table 2. Best-fit derived quantities for different values of $\eta_{\text{inj,p}}$, B_{RS} , and η_{mfp} .

$\eta_{\text{inj,p}}$	B_{RS} μG	η_{mfp}	r_{FS}	r_{RS}	V_{FS} km/s	V_{RS} km/s	ρ_0 amu/cm ³	D kpc	$E_{\text{SN}}(M_{\odot}/M_{\text{ej}})^{2/3}$ 10 ⁵¹ erg
0	—	—	4	4	4000	1700	0.67	5	0.3
$2 \cdot 10^{-4}$	5	1	14	13	12200	5800	0.23	15	9
10^{-3}	5	1	17	16	15800	7600	0.18	20	18
10^{-2}	5	1	18	17	18200	8800	0.17	23	30
$2 \cdot 10^{-4}$	25	15	10	7	6800	3100	0.39	8	1.7

ejecta (O, Ne, Mg, Si, S, Ar, Ca, and Fe). The derived values of FS and RS compression ratios (i.e., r_{FS} and r_{RS}), FS and RS speeds (V_{FS} and V_{RS}), ambient density, distance, and the energy-mass relation are, however, very different as shown in Table 2.

To get a temperature high enough to produce the iron K-line and the high energy continuum, all nonlinear fits require larger shock velocities and lower ambient densities. These imply more kinetic energy in the ejecta and a larger inferred distance, D , than the test-particle case.

The distance to Kepler is estimated to be 4.8 ± 1.4 kpc (Reynoso and Goss 1999). If the acceleration is efficient, this indicates that the acceleration parameters need to be modified. Using those derived from the fit to the radio synchrotron and X-ray continuum ($\eta_{\text{inj,p}} = 2 \cdot 10^{-4}$, $B_{\text{RS}} = 25 \mu\text{G}$, and $\eta_{\text{mfp}} = 15$, see Ellison 2000), the best-fit model (see Table 2.) places $\sim 4.6 \cdot 10^{51}$ erg in the shocked ejecta and ISM and of this, $\sim 38\%$ is in cosmic rays. The total energy estimate is high, but accounting for azimuthal variations in the data, or other effects, would reduce it.

Better constraints on all these parameters will be possible in the future by fitting radio and X-ray data simultaneously, from a specific region, with models which self-consistently include the nonthermal continuum. This continuum would replace the power law added to improve the X-ray fit by Decourchelle & Petre (1999), but is beyond the scope of this Letter.

5. CONCLUSION

Nonlinear effects from efficient particle acceleration strongly influence the thermal X-ray emission in SNRs,

and may serve as a tracer of cosmic ray acceleration. Here, we have focused on the consequences of shock acceleration on the thermal X-ray emission and have presented the first nonlinear, non-equilibrium ionization modeling of the X-ray emission from a specific SNR. While our self-similar approach has limitations which must be carefully considered, we believe it contains the essential physics and allows the exploration of a large range of parameters. We find that typical source parameters of young SNRs should result in significant nonlinear acceleration which, to fit the data, imply larger shock speeds and greater distances than test-particle models.

If cosmic ray production is efficient, shock *heating* is linked to particle *acceleration* and thus to the broadband photon emission from energetic electrons and ions. The high energy electrons produce both radio and X-ray synchrotron and this will be included in future work.

In addition to a possible nonthermal synchrotron component, regions undergoing strong acceleration should exhibit stronger and lower temperature thermal emission, while regions with little acceleration should be fainter and at a higher temperature.

Also, other complications (e.g., the variation of the ambient magnetic field orientation (Reynolds 1998), shock interactions with clouds and dense knots, etc.) influence the full modeling of SNRs. The spatially resolved spectra from the *Chandra* and *XMM-Newton* satellites should greatly aid the investigation of these and other effects.

We thank L. Drury, J. Hughes and E. Parizot for useful discussions as well as the referee for his helpful comments.

REFERENCES

Achterberg, A., Blandford, R. D., Reynolds, S. P. 1994, A&A, 281, 220
 Allen, G. E., et al. 1997, ApJ(Letts), 487, 97
 Arnaud, M., Raymond, J. 1992, ApJ, 398, 394
 Arnaud, M., Rothenflug, R. 1985, A&AS, 60, 425
 Berezhko, E. G., Ellison, D. C. 1999, ApJ, 526, 385
 Berezhko, E. G., Ksenofontov, L., & Petukhov, S. I. 1999, Proc. 26th ICRC (Salt Lake City), Vol. 4, p. 377. (OG 3.3.23)
 Blandford, R. D., & Eichler, D. 1987, Phys. Repts., 154, 1
 Borkowski, K. J., Rho, J., Reynolds, S. P., & Dyer, K. K. 2000, ApJ, submitted., astro-ph/0006149
 Boulares, A., & Cox, D. 1988, ApJ, 333, 198
 Chevalier, R. A. 1982, ApJ, 258, 790
 Chevalier, R. A. 1983, ApJ, 272, 765
 Decourchelle, A., & Ballet, J. 1994, A&A, 287, 206
 Decourchelle, A., & Petre, R. 1999, Astron. Nachr., 320, 203
 Decourchelle, A., et al. 2000, in preparation
 Dorfi, E. A., & Böhringer, H. 1993, A&A, 273, 251
 Drury, L. O. C. 1983, Rep. Prog. Phys., 46, 973
 Ellison, D. C. 2000, ACE proceedings paper, astro-ph/0003214
 Ellison, D. C., Berezhko, E. G., & Baring, M. G. 2000, ApJ, in press, astro-ph/0003188
 Ellison, D. C., Giacalone, J., Burgess, D., & Schwartz, S. J. 1993, J.G.R., 98, 21,085
 Heavens, A. F. 1984, M.N.R.A.S., 211, 195
 Hughes, J. P., Rakowski, C. E., & Decourchelle, A. 2000, ApJ(Letts), in press, astro-ph/0007032
 Jones, F. C., & Ellison, D. C. 1991, Space Sci. Rev., 58, 259-346
 Kang, H., & Jones, T. W. 1991, M.N.R.A.S., 249, 439
 Kinugasa, K., & Tsunemi, H. 1999, P.A.S.J., 51, 239
 Koyama, K., Petre, R., Gotthelf, E. V., Hwang, U., Matsuura, M., Ozaki, M., & Holt, S. S. 1995, Nature, 378, 255
 Mewe, R., Gronenschild, E. H. B. M., van den Oord, G. H. J. 1985, A&AS, 62, 197
 Mewe, R., Lemen, J. R., van den Oord, G. H. J. 1986, A&AS, 65, 511
 Meyer, J. P. 1985, ApJS, 57, 173
 Nadezhin, D. K. 1985, Astr. Sp. Sci., 112, 225
 Porquet, D., et al. 2000, in preparation
 Reynolds, S. P. 1998, ApJ, 493, 375
 Reynoso, E. M., Goss, W. M. 1999, AJ, 118, 926
 Slane, P., Gaensler, B. M., Dame, T. M., Hughes, J. P., Plucinsky, P. P., Green, A. 1999, ApJ, 525, 357
 Terasawa, T., et al. 1999, Proc. 26th Int. Cosmic Ray Conf. (Salt Lake City), 6, 528.